



Published in final edited form as:

Med Eng Phys. 2009 January ; 31(1): 10–16. doi:10.1016/j.medengphy.2008.03.003.

Validation of Three-Dimensional Model-Based Tibio-Femoral Tracking During Running

William Anderst^{*}, Roger Zauel[†], Jennifer Bishop[†], Erinn Demps[†], and Scott Tashman, Ph.D.^{*}

^{*} *University of Pittsburgh, Department of Orthopaedic Surgery, Pittsburgh, PA, USA*

[†] *Henry Ford Health System, Bone and Joint Center, Detroit, MI, USA*

Abstract

The purpose of this study was to determine the accuracy of a radiographic model-based tracking technique that measures the three-dimensional in vivo motion of the tibio-femoral joint during running. Tantalum beads were implanted into the femur and tibia of three subjects and CT scans were acquired after bead implantation. The subjects ran 2.5 m/s on a treadmill positioned within a biplane radiographic system while images were acquired at 250 frames per second. Three-dimensional implanted bead locations were determined and used as a “gold standard” to measure the accuracy of the model-based tracking. The model-based tracking technique optimized the correlation between the radiographs acquired via the biplane x-ray system and digitally reconstructed radiographs created from the volume-rendered CT model. Accuracy was defined in terms of measurement system bias, precision and rms error. Results were reported in terms of individual bone tracking and in terms of clinically relevant tibio-femoral joint translations and rotations (joint kinematics). Accuracy for joint kinematics was as follows: Model-based tracking measured static joint orientation with a precision of 0.2° or better, and static joint position with a precision of 0.2 mm or better. Model-based tracking precision for dynamic joint rotation was $0.9 \pm 0.3^\circ$, $0.6 \pm 0.3^\circ$, and $0.3 \pm 0.1^\circ$ for flexion-extension, external-internal rotation, and ab-adduction, respectively. Model-based tracking precision when measuring dynamic joint translation was 0.3 ± 0.1 mm, 0.4 ± 0.2 mm, and 0.7 ± 0.2 mm in the medial-lateral, proximal-distal, and anterior-posterior direction, respectively. The combination of high-speed biplane radiography and volumetric model-based tracking achieves excellent accuracy during in vivo, dynamic knee motion without the necessity for invasive bead implantation.

1. Introduction

Accurate in vivo joint motion data is necessary for numerous orthopaedic research applications, including tracking the development and progression of osteoarthritis, measuring joint function following surgery or rehabilitation, and providing input data to modeling applications. Biplane radiography (a.k.a. radiostereometric analysis, or RSA) is a promising data collection technique for these applications. Bone location and orientation can be precisely measured by beads implanted into the bones (bead-based)[1–3] or by matching a model to the radiographic images (model-based)[4–10].

The present study compares a previously validated bead-based method of tracking bone motion in vivo[11] to a new model-based method. The model-based method relies on a computer

Publisher's Disclaimer: This is a PDF file of an unedited manuscript that has been accepted for publication. As a service to our customers we are providing this early version of the manuscript. The manuscript will undergo copyediting, typesetting, and review of the resulting proof before it is published in its final citable form. Please note that during the production process errors may be discovered which could affect the content, and all legal disclaimers that apply to the journal pertain.

algorithm to maximize the correlation between biplane radiographic images and digitally reconstructed radiographs (DRRs). The DRRs are created by placing a volumetric model of the bone in a virtual biplane x-ray system identical to the laboratory system. Validation of this model-based tracking technique has been previously published for the study of gleno-humeral motion in cadaver specimens[5]. The present study expands on this work by collecting in vivo data during the dynamic activity of downhill running and presenting the accuracy results in terms of clinically relevant three-dimensional joint kinematics. The purpose of this study was to determine the accuracy of the model-based tracking procedure when measuring motion of the femur and tibia during a fast movement activity (downhill running), and to express these accuracy measures in terms of an anatomical coordinate system.

2. Materials and Methods

Subjects for this study were part of a larger study investigating knee kinematics after ACL reconstruction[12]. After obtaining informed consent, three 1.6 mm diameter spherical tantalum beads were implanted bilaterally into the femurs and tibias of each subject during ACL reconstruction surgery. Data used in this validation study were obtained solely from the ACL-intact leg of each subject.

Following sufficient healing and rehabilitation (4–6 months), bilateral computed tomography (CT) scans were collected with slice spacing of 1.25 mm, 28 cm field of view and 512×512 pixels per image (0.547 mm/pixel in-plane resolution). Tantalum bead locations were identified in the CT scans. Bead signatures were then manually removed from the CT slices by replacing pixels containing bead signal with pixels containing surrounding bone tissue so they would not influence model-based tracking results. The femur and tibia were segmented by a combination of thresholding and manual segmentation. The CT volume (defined as the outer cortical bone surface plus all interior bone tissue) was interpolated to create nearly cubic voxels with dimensions $0.273 \times 0.273 \times 0.250$ mm. This oversampling facilitated the use of a computationally efficient “nearest neighbor” rule when creating the DRR projections (as opposed to a tri-linear interpolation of 0.5^3 mm voxels).

Subjects were tested while standing on level ground and while running on a treadmill (2.5 m/s) set at a 10° decline (because it is believed downhill running increases the demands placed on the ACL). One standing and three running trials were collected for each subject. Biplane radiographic data was collected at 250 images per second by high-speed cameras (Phantom IV, Vision Research). The cameras were optically coupled to image intensifiers (Shimadzu Medical Systems) and shuttered at 1/2000 s to eliminate motion blur. Radiographic parameters were optimized to identify the implanted beads (90 kV, 100 mA). Maximum entrance exposure from the biplane radiographic system using these parameters was 0.24 R per trial. Subjects ran directly toward one image intensifier/camera while the other image intensifier/camera was approximately 45° lateral to the treadmill belt direction (Figure 1). This arrangement maximized the time the knee was within the imaging volume and minimized the interference from the contralateral leg. A calibration object defined the laboratory-based coordinate system, with the x-axis directed between the two image intensifiers, the z-axis directed vertically, and the y-axis perpendicular to both the x and z-axis (Figure 1). The direction of this lab-based coordinate system was not precisely controlled for this study because the lab-based coordinate system orientation is not relevant when results are reported in an anatomical-based coordinate system defined by bone landmarks.

The calibration object was also used to determine the precise location of the two high-speed cameras and x-ray sources during data collection. A custom computer program then recreated the 3D location and orientation of the high-speed cameras and x-ray sources within the computer to create a virtual test configuration identical to the actual biplane radiographic

imaging system. Given the x-ray source and camera locations, a digitally reconstructed radiograph (DRR) was created by placing the CT bone volume in the virtual testing configuration. As the CT volume was translated and rotated within the virtual testing configuration, the DRRs changed accordingly. The DRRs overlaid the distortion corrected biplane radiographic data and provided visual feedback to the operator regarding the similarity between the DRRs and radiographic images (Figure 2). Initially, the operator interactively positioned the CT volume reconstruction in two consecutive frames. Custom computer code used these initial estimates to begin a search to optimize the correlation between the DRRs and radiographic images. Once the optimum correlation was calculated, the computer program performed the same optimization procedure for successive frames, using a linear extrapolation of previously solved frames as the initial guess for each unsolved frame. Extensive details of this computerized matching procedure for model-based tracking have been previously published[5]. To briefly summarize, the product of the correlation coefficients of the two DRRs with their respective radiographs was the objective function. The correlation was calculated only in the actual footprint of the DRR. The time required for each iteration in the matching process varied depending on many factors, however, a recent test revealed an average time of 4.6 seconds per frame, with an average of 4.3 search iterations and 180 DRRs calculated per frame. These values were obtained with a CT object size of $373 \times 289 \times 654$ voxels and a ray-sampling interval of 0.75 mm using 512×512 radiographic images. A cluster of 24 computers using parallel processing performed these calculations.

Implanted beads were tracked in the distortion corrected radiographs as described previously [11]. The accuracy of tracking implanted beads was determined by calculating the bias and precision in inter-bead distances within each bone over the entire dynamic trial, using procedures identical to those previously published[11], with bias defined as the average difference in intermarker bead spacing determined using either CT slices or radiographs for each frame of an entire trial. Precision was defined as the standard deviation of these differences over the entire trial. Bead-based tracking was then used as the “gold standard” to calculate the accuracy of the model-based tracking. Raw, unfiltered bead-based and model-based tracking results were compared for the lab-based coordinate system validation. All raw data were then filtered at 20 Hz using a fourth-order, low-pass Butterworth filter to calculate joint kinematics in an anatomical coordinate system. Data from foot touchdown to 0.2 s after touchdown were compared for the kinematic validation, as this was the point at which occlusion from the contralateral leg began to occur. Standing trials consisted of a sequence of 25 frames of data with image parameters (kv, mA, exposure time) identical to those for the running trials.

For each frame of every trial, the centroid of the three implanted beads was calculated for each bone using both the bead-based and model-based tracking technique. Agreement between the two systems was quantified by bias (average difference in center of bead locations over the entire trial) and precision (standard deviation of differences over the entire trial). Root-mean-squared error (the rms difference between the two techniques across the entire trial) was also calculated to compare with previously published results. Average accuracy measures were calculated for the femur and tibia of each subject (one standing trial per subject; subject A and C: three dynamic trials, subject B: two dynamic trials). Mean accuracy values for the three individual subjects were averaged to determine system accuracy in tracking individual bones and expressed in the laboratory-based coordinate system.

Clinically relevant joint kinematics were calculated from each of the bead-based and model-based tracking results. Drill holes for the ACL grafts were identified in the surgically reconstructed joint and mirror imaged onto the healthy joint investigated in the present study. Drill hole locations indicated ACL attachment sites on the femur and tibia. Translation was defined as the 3D distance between the femur and tibia ACL attachment sites, and expressed in the tibia anatomical coordinate system. Rotations were calculated using ordered rotations

[13]. Anatomic coordinate systems were defined as described previously[3]. Accuracy measures (bias, precision, rms error) for clinically relevant kinematic variables were calculated as described above for the 200 ms following foot touchdown. One-sample, two-tailed, t-tests with alpha set at 0.05 were used to test for bias in all cases.

Model-based tracking accuracy may be related to the velocity of the objects being tracked due to within-image motion blur. Therefore, the average absolute value of the lab-based x, y and z-axis velocity components of the center of the three beads was determined for each trial.

3. Results

There was no bias in implanted bead tracking (the “gold standard”) for either the static or dynamic trials (Table 1). Femur bead tracking precision was similar to tibia bead tracking precision for the static and dynamic trials, however tracking precision was approximately 2.5 times better for static trials compared to dynamic trials (Table 1).

For individual bone tracking, model-based tracking bias for static trials was significant only for the tibia in the lab-based z-direction (Table 2A). Model-based precision for static trials ranged from 0.030 to 0.080 mm, depending on laboratory axis direction, with x-axis measurements less precise than y-axis and z-axis measurements (Table 2A). Femur and tibia tracking precision values were similar.

Model-based tracking bias for individual bones during dynamic trials was not significant for either bone in any lab-based coordinate system direction (Table 2B). Model-based tracking precision for dynamic trials ranged from 0.15 to 0.52 mm, depending on laboratory axis direction, with x-axis precision worse than y-axis and z-axis precision by a factor of approximately two (Table 2B). Precision was not bone-dependent.

Static and dynamic measurement bias was not significantly different from zero for any anatomical coordinate system joint rotation or translation (Table 3A, Table 3B). Kinematic measurement precision ranged from 0.06° to 0.21° for static trial rotations and from 0.34° to 1.27° for dynamic trial rotation measurements. Kinematic measurement precision ranged from 0.09 mm to 0.19 mm for static trial translations and from 0.31 mm to 0.74 mm for dynamic trial translation measurements. Similarly, rms errors were larger for dynamic trials than static trials (Table 3A, Table 3B). Variability in kinematics between trials was low, and within trial differences between the two tracking techniques were small (Figure 3, Figure 4).

The average absolute value of the lab-based velocity components of the center of the three beads was 0.46 ± 0.17 m/s, 0.15 ± 0.08 m/s, and 0.46 ± 0.30 m/s in the x, y and z-directions, respectively, for the femur, and 0.48 ± 0.17 m/s, 0.18 ± 0.02 m/s, 0.49 ± 0.26 m/s in the x, y and z-directions, respectively, for the tibia. The average peak lab-based velocity components of the center of the three beads was 1.26 ± 0.37 m/s, 0.41 ± 0.22 m/s, and 0.77 ± 0.13 m/s in the x, y, and z-directions, respectively for the femur, and 1.32 ± 0.14 m/s, 0.48 ± 0.16 m/s, 0.84 ± 0.18 m/s in the x, y and z-directions, respectively, for the tibia.

4. Discussion

Implanted bead tracking, the gold standard, was extremely precise for static measurements (0.04 mm). However, dynamic tracking of the beads was less precise than previously reported [11] (0.12 mm compared to 0.07 mm). This was most likely due to the higher density tissues imaged (human vs. canine knees) and an increase in occlusion-producing materials such as external surface markers and electrode wires. The human knee is surrounded by much more tissue than the canine knee, leading to decreased contrast between implanted beads and

surrounding tissues. As a result, the computer algorithm located tantalum bead centers with less precision.

Comparing model-based tracking of individual bones to the “gold standard”, precision values in the lab-based x-axis direction were approximately two times higher than those in the y and z-axis directions, indicating less precision in the x-axis measurements for both the static and dynamic trials. Model-based matching techniques are most imprecise when measuring movement perpendicular to the radiographic image plane[14–16]. In the present study, the subjects ran directly toward one imaging plane, which, by coincidence, was closely aligned with the laboratory-based x-axis direction. Although the movement speed in the x and z-directions was high compared to the y-axis direction, the precision in the z-direction was as good as the precision in the lab-based y-direction, and this held for both the static and dynamic trials (Table 2A, Table 2B). Thus, it appears measurements in the lab-based x-axis direction were the least precise due to the relationship between the imaging planes and the primary direction of movement. It is also possible peak movement velocity may have affected precision measures. Given a peak movement speed of 1.3 m/s and an exposure time of .5 ms, the associated motion blur could be as high as 0.65 mm (if the motion was parallel to the image plane).

The femur tracking precision was noticeably worse in one of the three subjects (Subject A). The average dynamic trial precision for this subject was 1.01 mm, 0.41 mm and 0.422 mm for the x, y, and z-directions, respectively. These measures were three to four times worse than the other two subjects, who had an average femur tracking precision of 0.27 mm, 0.14 mm and 0.12 mm for the x, y, and z-directions, respectively. The decreased precision was likely due to a shorter CT scan acquired from Subject A (68.75 mm in length versus 78.75 mm and 150 mm for subjects B and C, respectively). Also, differences between bead-based and model-based results for Subject A were most apparent near the end of the motion sequence, at a time when occlusion from the contralateral leg was greatest. These results show that even slightly increasing the amount of bone within the volumetric CT reconstruction is beneficial to model-based tracking.

The objective of model-based tracking is to obtain accurate three-dimensional kinematic measurements of the joint (the tibia relative to the femur, or vice versa), not simply the three-dimensional location of an individual bone. Individual femur and tibia model-based tracking results can be combined to determine the clinically relevant joint kinematic accuracy (Table 3). This reveals the accuracy that can be expected during application of model-based tracking. Precision values were outstanding for the static trials (0.21° or better in rotation and 0.19 mm or better in translation), and very good for the dynamic trials (0.94° or better in rotation and 0.74 mm or better in translation). Note that the most imprecise translation measures were in the anterior-posterior direction, roughly the direction of the treadmill belt and the lab-based x-axis direction. It is possible AP precision may be improved by increasing the angle between the image planes and changing the primary direction of movement relative to the image planes. These results indicate the model-based tracking technique can be a useful tool for investigating in vivo dynamic knee joint function with sub-millimeter accuracy. Although this technique provides highly accurate three-dimensional kinematic input data that could be used in finite element modeling dynamic in vivo movement, it should be noted that the high accuracy reported here is still larger than perturbations that dramatically affect finite element model results [17].

There are several limitations to the current study. First, the “gold standard” measurement was shown to have a precision of 0.12 mm. Ideally, the accuracy of the reference standard should be an order of magnitude better than the accuracy of the technique being validated. However, in this case, it was believed it was better to validate the model-based technique during a high-

speed, dynamic motion in vivo with a gold standard of “only” 0.12 mm rather than devise a test arrangement unlike the conditions that will be in place during the application of this technique. Secondly, the radiographic images used in the current validation study were not optimized for the model-based tracking technique. Rather, the images were optimized for maximum contrast between implanted beads and surrounding tissues. This resulted in some bone edges occasionally being “washed out” in the radiographic images on one or both cameras. Tracking accuracy should improve with appropriate contrast and exposure in the radiographic images. A third limitation involves the CT models. CT scans were collected for two of the present subjects without regard for their use in model-based tracking. Thus, the CT scans included relatively short portions of the femur and tibia, just enough to include each of the implanted tantalum beads. As discussed above, increased accuracy may be achieved by increasing the distance along the shaft of each bone when collecting CT data. Additionally, CT segmentation parameters (threshold value, manual segmentation) may affect results. However, the use of a volumetric CT model for matching purposes reduces the influence of voxels identified (or misidentified) as bone cortex. The present technique passes rays through each voxel containing bone tissue to create the DRRs—not just the outer cortex as occurs when a surface CT model is used. Therefore, segmentation affects only a small proportion of the total number of voxels used to create the DRRs. Finally, in order to minimize occlusion of the stance leg during touchdown and initial weight bearing, the angle between cameras was set to only 45°. This relatively small angle between cameras may have slightly decreased three-dimensional accuracy. Clearly, there are numerous parameters that can affect model-based tracking accuracy, including bone under investigation, CT segmentation, CT reconstruction size, camera location, radiographic parameters (kV and mA), movement velocity, and exposure time. A future study will be necessary to determine the effects of each of these parameters on model-based tracking accuracy.

Matching radiographic images with simulated images from bone or implant models is a popular technique for precisely measuring in vivo kinematics. In some cases, single plane radiographs are collected and three-dimensional kinematics are calculated [14–16]. These 2D to 3D measurements have poor accuracy for measurements out of the radiographic image plane. Other researchers collect biplane radiographs to study static [6,7,18] or dynamic [3,19] activities. It is important to note the methods used to validate these measurement techniques. Previous validation attempts have included imaging stationary metallic objects[9], manual matching procedures[7,9,18], and no comparison to a gold standard[6]. Impressive accuracy results are irrelevant if the methods by which these results were acquired are not appropriate for the intended application of the technique. For example, algorithms devised for matching metallic objects to static fluoroscopic images are unlikely to perform adequately when dynamic motion of in vivo bones is under investigation. The present study, for instance, revealed individual bone tracking precision improved by nearly an order of magnitude when tracking static trials compared to dynamic trials (Table 2A and Table 2B) in spite of using identical imaging and radiographic parameters (exposure time, kV, mA). It is not always clear what radiographic and imaging parameters were used in previously published validation attempts. Regardless, the accuracy values reported for static validation techniques cannot be assumed to hold for data collected during dynamic motion, nor can accuracy results for metallic implant components be applied to bones.

Appropriate validation includes data collected under real-world testing conditions (e.g. in vivo, dynamic motion), comparison with a “gold standard” measurement, and evidence of the accuracy of the system, stating, at a minimum, the system bias and precision[20]. Validation of the present method was performed by static and dynamic in vivo testing, with imaging parameters identical to the intended application of the new tracking technique. It is incumbent upon researchers and the biomechanics community to insist on appropriately validated methods prior to the publication of results.

Acknowledgements

This work was supported by National Institutes of Health Grant AR46387.

References

1. Karrholm J, Selvik G, Elmqvist L, Hansson L, Jonsson H. Three-dimensional instability of the anterior cruciate deficient knee. *The Journal of Bone and Joint Surgery (Br)* 1988;70-B:777–783.
2. Selvik G. Roentgen Stereophotogrammetric Analysis. *Acta Radiol* 1990;31:113–126. [PubMed: 2196921]
3. Tashman S, Collon D, Anderson K, Kolowich P, Anderst W. Abnormal rotational knee motion during running after anterior cruciate ligament reconstruction. *American Journal of Sports Medicine* 2004;32(4):975–983. [PubMed: 15150046]
4. Berhonnaud E, Herzberg G, Zhao K, An K, Dimnet J. Three-dimensional in vivo displacements of the shoulder complex from biplanar radiography. *Surg Radiol Anat* 2005;27:214–222. [PubMed: 15789137]
5. Bey M, Zael R, Brock S, Tashman S. Validation of a new model-based tracking technique for measuring three-dimensional, in vivo glenohumeral joint kinematics. *Journal of Biomechanical Engineering* 2006;128(4):604–609. [PubMed: 16813452]
6. Bingham J, Li G. An optimized image matching method for determining in-vivo tka kinematics with a dual-orthogonal fluoroscopic imaging system. *Journal of Biomechanical Engineering* 2006;128(4):588–595. [PubMed: 16813450]
7. Hanson G, Suggs J, Freiberg A, Durbhakula S, Li G. Investigation of in vivo 6dof total knee arthroplasty kinematics using a dual orthogonal fluoroscopic system. *Journal of Orthopaedic Research* 2006;24(5):974–981. [PubMed: 16596640]
8. Lemieux L, Jagoe R, Fish D, Kitchen N, Thomas D. A patient-to-computed-tomography image registration method based on digitally reconstructed radiographs. *Medical Physics* 1994;21(11):1749–1760. [PubMed: 7891637]
9. Li G, Wuerz T, DeFrate L. Feasibility of using orthogonal fluoroscopic images to measure in vivo joint kinematics. *Journal of Biomechanical Engineering* 2004;126(2):314–318. [PubMed: 15179865]
10. You B, Siy P, Anderst W, Tashman S. In vivo measurement of 3-D skeletal kinematics from sequences of biplane radiographs: application to knee kinematics. *IEEE Trans Med Imaging* 2001;20(6):514–525. [PubMed: 11437111]
11. Tashman S, Anderst W. In-vivo measurement of dynamic joint motion using high speed biplane radiography and CT: application to canine ACL deficiency. *Journal of Biomechanical Engineering* 2003;125(2):238–245. [PubMed: 12751286]
12. Tashman S, Kolowich P, Collon D, Anderson K, Anderst W. Dynamic function of the acl-reconstructed knee during running. *Clinical Orthopaedics and Related Research* 2007;454:66–73. [PubMed: 17091011]
13. Grood E, Suntay W. A joint coordinate system for the clinical description of three-dimensional motions: application to the knee. *Journal of Biomedical Engineering* 2007;105(2):136–144.
14. Banks S, Hodge W. Accurate measurement of three-dimensional knee replacement kinematics using single plane fluoroscopy. *IEEE Transactions on Biomedical Engineering* 1996;43(6):638–649. [PubMed: 8987268]
15. Dennis D, Mahfouz M, Komistek R, Hoff W. In vivo determination of normal and anterior cruciate ligament-deficient knee kinematics. *Journal of Biomechanics* 2005;38:241–253. [PubMed: 15598450]
16. Mahfouz M, Hoff W, Komistek R, Dennis D. A robust method for registration of three dimensional knee implant models to two-dimensional fluoroscopy images. *IEEE Transactions on Medical Imaging* 2003;22(12):1561–1574. [PubMed: 14649746]
17. Yao J, Salo A, Lee J, Lerner A. Sensitivity of tibio-menisco-femoral joint contact behavior to variations in knee kinematics. *Journal of Biomechanics* 2008;41:390–398. [PubMed: 17950743]
18. Li G, Moses J, Papannagari R, Pathare N, DeFrate L, Gill T. Anterior cruciate ligament deficiency alters the in vivo motion of the tibiofemoral cartilage contact points in both the anteriorposterior and

- mediolateral directions. *Journal of Bone and Joint Surgery* 2006;88-A(8):1826–1834. [PubMed: 16882908]
19. Tashman S, Anderst W, Kolowich P, Havestad S, Arnoczy S. Kinematics of the ACL-deficient canine knee during gait: serial changes over two years. *Journal of Orthopaedic Research* 2004;22(5):931–941. [PubMed: 15304262]
 20. ASTM. Standard practice for use of the terms precision and bias in ASTM test methods. West Conshohocken, PA: 1996.

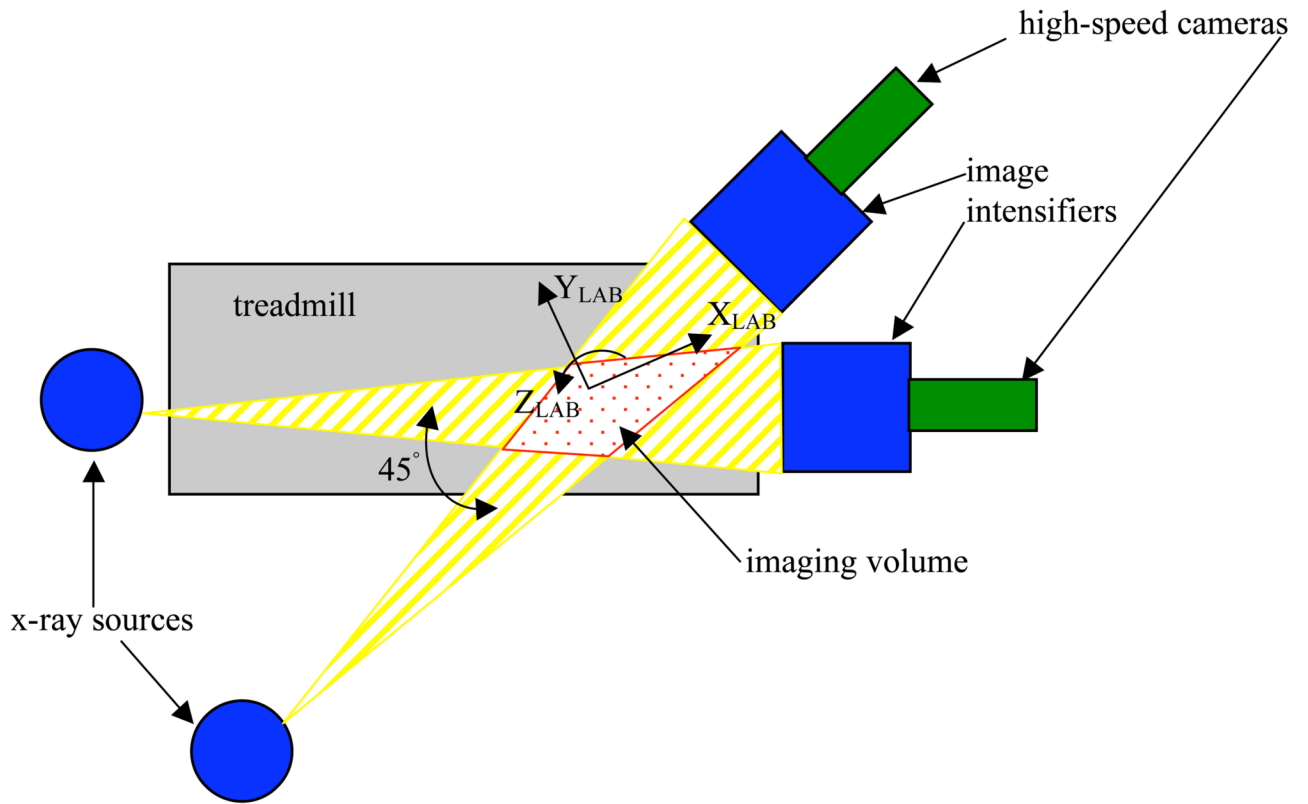


Figure 1.

Overhead view of the biplane radiographic system. Subjects ran on treadmill toward image intensifiers with the study leg within the imaging volume shortly before and after footstrike. The laboratory coordinate system was defined by a control object placed within the imaging volume (x-axis directed between image intensifiers, y-axis directed perpendicular to x-axis in the horizontal plane, and z-axis vertical).

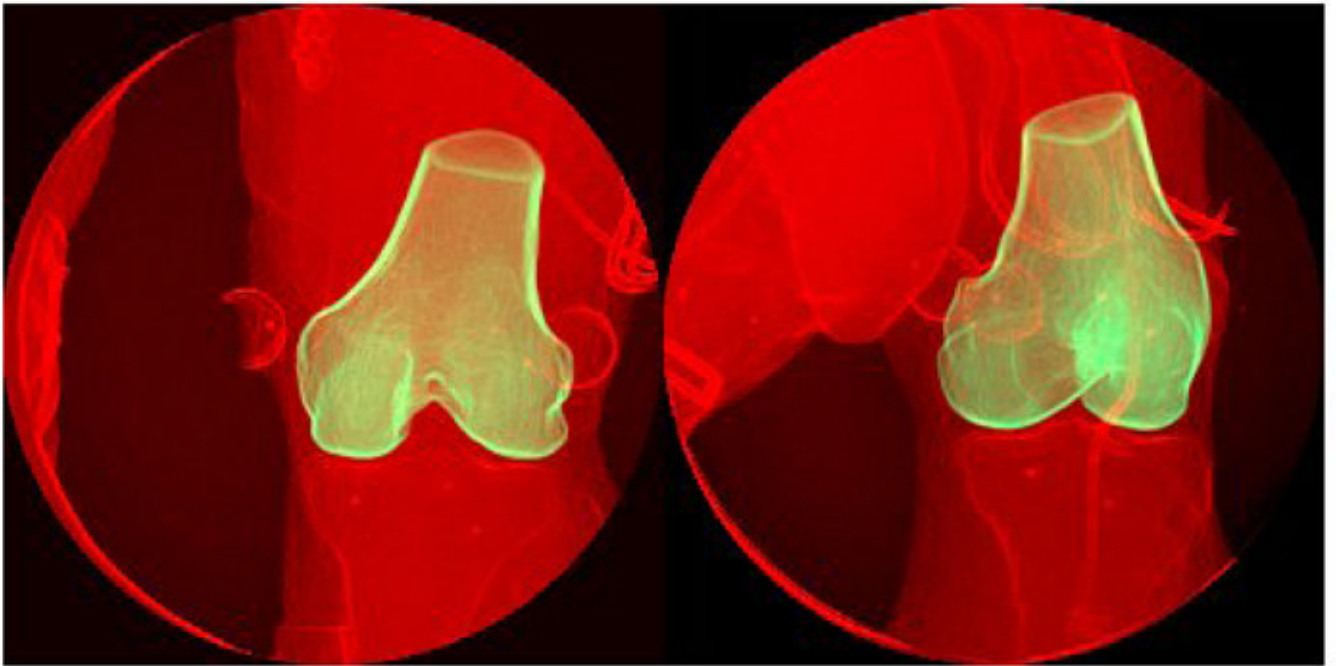


Figure 2. Digitally reconstructed radiograph (DRR) of the femur (yellow) superimposed on distortion corrected biplane radiographs (red). Note implanted beads are not present in DRR. External surface markers and electrode wires are also visible in biplane radiographs.

Flexion-Extension Measurements

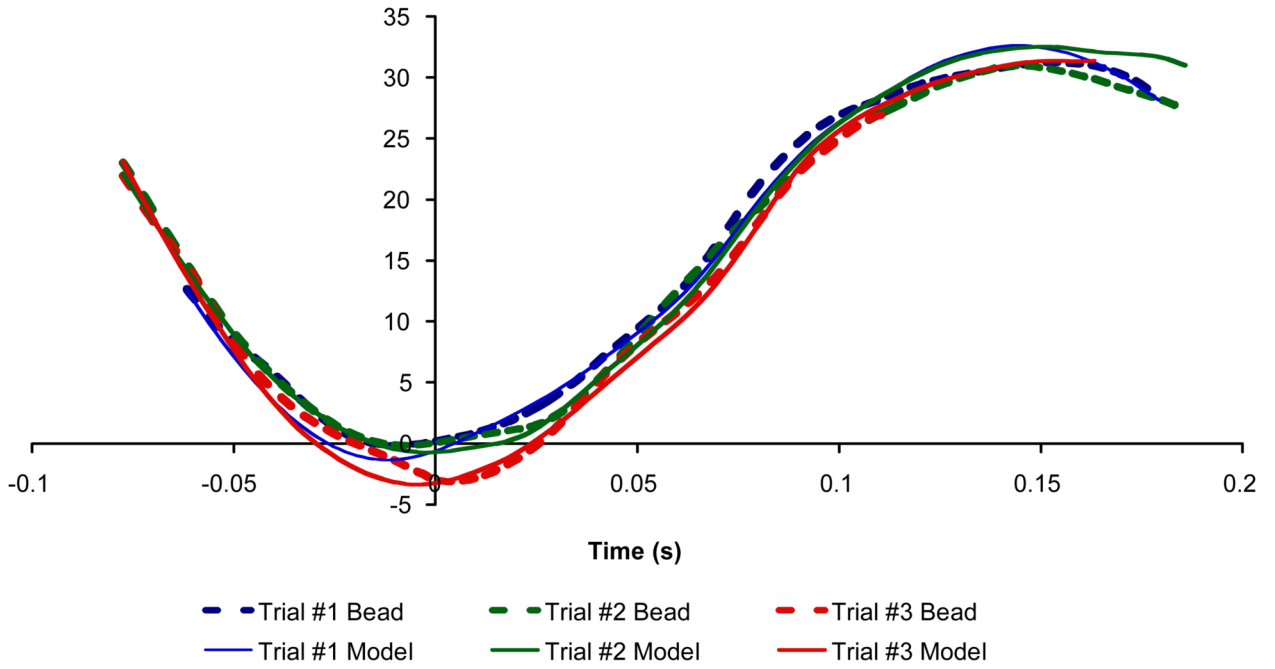


Figure 3. Flexion-extension plots for three trials of Subject C. Bead-based tracking curves are dashed lines, model-based tracking results are solid lines. Horizontal axis is time relative to foot touchdown, vertical axis is flexion angle.

Anterior-Posterior Translation Measurements

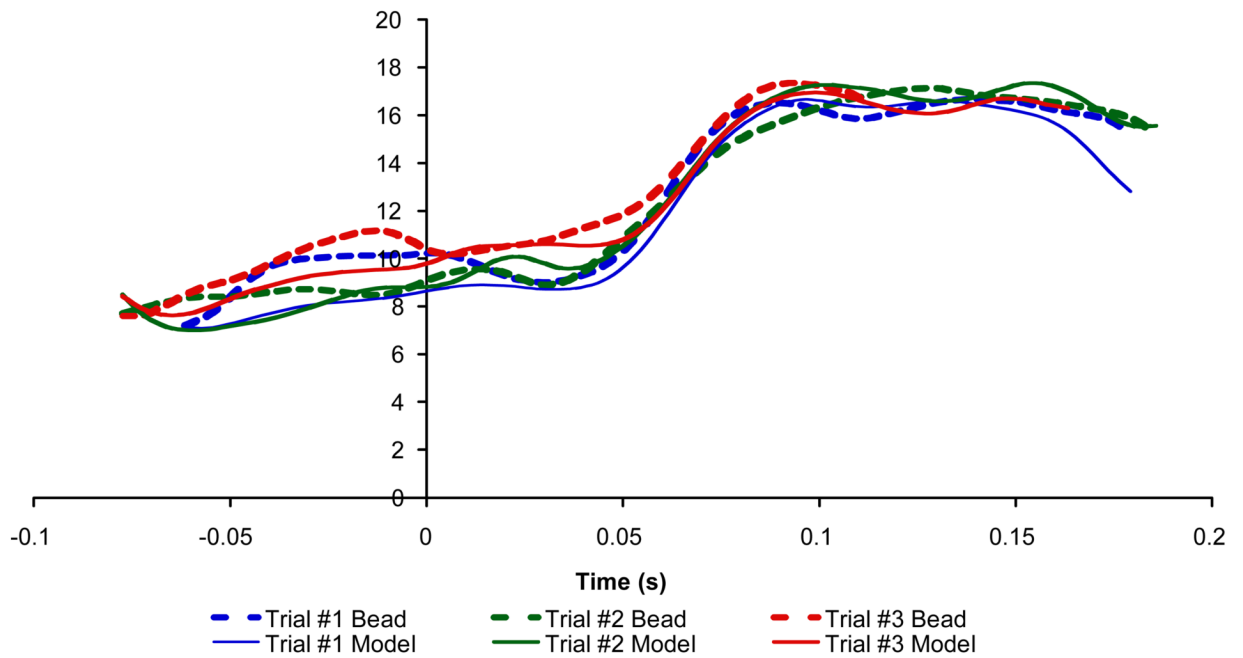


Figure 4.

Anterior-posterior translation plots for three trials of Subject C. Bead-based tracking curves are dashed lines, model-based tracking results are solid lines. Horizontal axis is time relative to foot touchdown, vertical axis is flexion angle.

Bead-based tracking accuracy (bias and precision). All units in mm. All bias measures not significantly different from zero.

Table 1

| Data Collection Mode | Bone | Bias | Precision |
|-----------------------------|-------------|--------------|------------------|
| Static | Femur | -0.02 ± 0.18 | 0.04 ± 0.02 |
| Static | Tibia | 0.08 ± 0.19 | 0.04 ± 0.01 |
| Dynamic | Femur | -0.07 ± 0.13 | 0.12 ± 0.01 |
| Dynamic | Tibia | 0.08 ± 0.14 | 0.12 ± 0.01 |

Explanation of table data: For each trial, between-bead distances were calculated within each bone for each data frame. This time history of interbead-distances was used to calculate mean difference between inter-bead distances calculated from CT slice data and biplane radiographic image data (bias) and standard deviation of these differences (precision). Data from all trials from the same subject were averaged to obtain a single average for each subject. The averages of all subjects were then calculated and appear in this table.

Table 2

Table 2A Model-based tracking accuracy for individual bones (bias, precision, rms error): Static trials. All units in mm.

| Axis | Bias | | | Precision | | | rms error | | |
|------|--------------|---------------|-------|-------------|-------------|-------|-------------|-------|-------------|
| | Femur | Tibia | Tibia | Femur | Tibia | Tibia | Femur | Tibia | Tibia |
| x | -0.01 ± 0.51 | -0.14 ± 0.47 | | 0.07 ± 0.02 | 0.08 ± 0.04 | | 0.18 ± 0.16 | | 0.17 ± 0.06 |
| y | -0.14 ± 0.18 | 0.14 ± 0.24 | | 0.04 ± 0.02 | 0.03 ± 0.14 | | 0.04 ± 0.04 | | 0.06 ± 0.05 |
| z | -0.18 ± 0.54 | -0.37 ± 0.13* | | 0.04 ± 0.02 | 0.04 ± 0.01 | | 0.23 ± 0.30 | | 0.15 ± 0.10 |

Table 2B Model-based tracking accuracy for individual bones (bias, precision, rms error): Dynamic trials. All units in mm. All bias measures not significantly different from zero.

| Axis | Bias | | | Precision | | | rms error | | |
|------|--------------|--------------|-------|-------------|-------------|-------|-------------|-------|-------------|
| | Femur | Tibia | Tibia | Femur | Tibia | Tibia | Femur | Tibia | Tibia |
| x | -0.22 ± 0.15 | -0.68 ± 0.84 | | 0.52 ± 0.43 | 0.45 ± 0.09 | | 0.60 ± 0.48 | | 0.88 ± 0.74 |
| y | -0.01 ± 0.11 | 0.32 ± 0.48 | | 0.22 ± 0.16 | 0.15 ± 0.06 | | 0.23 ± 0.12 | | 0.41 ± 0.40 |
| z | -0.06 ± 0.36 | -0.10 ± 0.25 | | 0.22 ± 0.18 | 0.26 ± 0.14 | | 0.32 ± 0.19 | | 0.32 ± 0.12 |

* = different from zero, alpha = 0.05

Explanation of table data: For each trial, the difference in bead centroid location between the bead-based method and the model-based method was calculated for each data frame. This time history of differences was used to calculate mean difference between methods (bias) and standard deviation of these differences (precision). Data from all trials from the same subject were averaged to obtain a single average for each subject. The averages of all subjects were then calculated and appear in this table.

Table 3

Table 3A Model-based kinematic measurement accuracy (bias, precision, rms error): Static trials. All bias measures not significantly different from zero.

| Measurement | Bias | Precision | rms error |
|--------------------------------|------------------------|-----------------------|-----------------------|
| Flexion-extension | $0.60 \pm 1.03^\circ$ | $0.21 \pm 0.04^\circ$ | $0.85 \pm 0.76^\circ$ |
| External-Internal rotation | $0.31 \pm 0.88^\circ$ | $0.16 \pm 0.09^\circ$ | $0.67 \pm 0.58^\circ$ |
| Ab-Adduction | $-0.30 \pm 0.27^\circ$ | $0.06 \pm 0.03^\circ$ | $0.28 \pm 0.27^\circ$ |
| Medial-Lateral Translation | -0.21 ± 0.25 mm | 0.09 ± 0.02 mm | 0.24 ± 0.15 mm |
| Proximal-Distal Translation | -0.19 ± 0.11 mm | 0.09 ± 0.06 mm | 0.18 ± 0.04 mm |
| Anterior-Posterior Translation | -0.08 ± 0.28 mm | 0.19 ± 0.06 mm | 0.26 ± 0.07 mm |

Table 3B Model-based kinematic measurement accuracy (bias, precision, rms error): Dynamic trials. All bias measures not significantly different from zero.

| Measurement | Bias | Precision | rms error |
|--------------------------------|------------------------|-----------------------|-----------------------|
| Flexion-extension | $-0.30 \pm 0.80^\circ$ | $0.94 \pm 0.29^\circ$ | $1.75 \pm 0.61^\circ$ |
| External-Internal rotation | $1.01 \pm 2.04^\circ$ | $0.62 \pm 0.27^\circ$ | $1.44 \pm 1.23^\circ$ |
| Ab-Adduction | $-0.11 \pm 0.53^\circ$ | $0.30 \pm 0.10^\circ$ | $0.54 \pm 0.20^\circ$ |
| Medial-Lateral Translation | -0.49 ± 0.81 mm | 0.31 ± 0.130 mm | 0.69 ± 0.46 mm |
| Proximal-Distal Translation | -0.16 ± 0.47 mm | 0.37 ± 0.16 mm | 0.69 ± 0.31 mm |
| Anterior-Posterior Translation | -0.68 ± 0.54 mm | 0.74 ± 0.20 mm | 1.54 ± 0.69 mm |

Explanation of table data: For each trial, the difference in kinematic measurements between the bead-based method and the model-based method was calculated for each data frame. This time history of differences was used to calculate mean difference between methods (bias) and standard deviation of these differences (precision). Data from all trials from the same subject were averaged to obtain a single average for each subject. The averages of all subjects were then calculated and appear in this table.